

# CHEMISTRY

## A European Journal

A Journal of



### Accepted Article

**Title:** Role of relative humidity and Cd/Zn stoichiometry in the photo-oxidation process of cadmium yellows ( $\text{CdS}/\text{Cd}_{1-x}\text{Zn}_x\text{S}$ ) in oil paintings

**Authors:** Letizia Monico, Annalisa Chieli, Steven De Meyer, Marine Cotte, Wout de Nolf, Gerald Falkenberg, Koen Janssens, Aldo Romani, and Costanza Miliani

This manuscript has been accepted after peer review and appears as an Accepted Article online prior to editing, proofing, and formal publication of the final Version of Record (VoR). This work is currently citable by using the Digital Object Identifier (DOI) given below. The VoR will be published online in Early View as soon as possible and may be different to this Accepted Article as a result of editing. Readers should obtain the VoR from the journal website shown below when it is published to ensure accuracy of information. The authors are responsible for the content of this Accepted Article.

**To be cited as:** *Chem. Eur. J.* 10.1002/chem.201801503

**Link to VoR:** <http://dx.doi.org/10.1002/chem.201801503>

Supported by  
**ACES**

WILEY-VCH

# Role of relative humidity and Cd/Zn stoichiometry in the photo-oxidation process of cadmium yellows (CdS/Cd<sub>1-x</sub>Zn<sub>x</sub>S) in oil paintings

Letizia Monico,<sup>\*,[a,b,c]</sup> Annalisa Chieli,<sup>[a,b]</sup> Steven De Meyer,<sup>[c]</sup> Marine Cotte,<sup>[d,e]</sup> Wout de Nolf,<sup>[d]</sup> Gerald Falkenberg,<sup>[f]</sup> Koen Janssens,<sup>[c]</sup> Aldo Romani,<sup>[a,b]</sup> Costanza Miliani<sup>\*,[b,a]</sup>

**Abstract:** Cadmium yellows (CdYs) refer to a family of cadmium sulfide pigments which have been widely used by artists since the late 19th century. Despite being considered stable, they are suffering from discoloration in iconic paintings, such as *Joy of Life* by Matisse, *Flowers in a blue vase* by Van Gogh and *the Scream* by Munch, most likely due to the formation of CdSO<sub>4</sub>·nH<sub>2</sub>O.

Questions about what the factors driving the CdYs degradation are and how they affect the overall process are still open.

Here, we study a series of oil mock-up paints made of CdYs of different stoichiometry (CdS/Cd<sub>0.76</sub>Zn<sub>0.24</sub>S) and crystalline structure (hexagonal/cubic) before and after aging at variable relative humidity under exposure to light and in darkness. Synchrotron-based X-ray methods combined with UV-Visible and FTIR spectroscopies show that: (i) Cd<sub>0.76</sub>Zn<sub>0.24</sub>S is more susceptible to photo-oxidation than CdS; both compounds can act as photocatalysts for the oil oxidation. (ii) The photo-oxidation of CdS/Cd<sub>0.76</sub>Zn<sub>0.24</sub>S to CdSO<sub>4</sub>·nH<sub>2</sub>O is triggered by moisture. (iii) The nature of alteration products depends on the aging conditions and Cd/Zn stoichiometry.

Based on our findings, we propose a scheme for the mechanism of the photocorrosion process and photocatalytic activity of CdY pigments in the oil binder.

Overall, our results form a reliable basis for understanding the degradation of CdS-based paints in artworks and contribute towards developing better ways of preserving them for future generations.

## Introduction

Since the late 19th century, cadmium sulfide (CdS) n-type semiconductors of different crystalline structures (hexagonal, cubic or amorphous) and Cd<sub>1-x</sub>Zn<sub>x</sub>S solid solutions (with 0 < x < 0.25–0.3) have been employed as yellow artists' pigments, forming the class of cadmium yellows (henceforth denoted as

CdYs).<sup>[1–3]</sup> These materials were frequently employed by prominent 19th–20th century painters, including Claude Monet,<sup>[4]</sup> Vincent van Gogh,<sup>[5]</sup> Georges Seurat,<sup>[6]</sup> James Ensor,<sup>[7]</sup> Edvard Munch,<sup>[8]</sup> Henri Matisse,<sup>[1,9]</sup> Piet Mondrian,<sup>[10]</sup> Pablo Picasso,<sup>[11]</sup> and Jackson Pollock.<sup>[12]</sup> Unfortunately, several iconic artworks by these masters suffer from the fading of the yellow paints. The phenomenon occasionally occurs along with the presence of superficial gray/ivory crusts and/or changes of the mechanical/morphological properties of the paint, such as chalking, flaking and crumbling.<sup>[5,7,9,13]</sup>

Over the last decade, the capabilities of synchrotron radiation (SR)-based micro-FTIR imaging and X-ray spectromicroscopic methods [i.e., micro X-ray diffraction (μ-XRD), micro X-ray absorption near edge structure (μ-XANES) and micro X-ray fluorescence (μ-XRF)] to provide spatially resolved elemental speciation and molecular information at the (sub)micrometer scale were exploited for studying the CdY paints discoloration in masterpieces by Van Gogh,<sup>[5]</sup> Ensor<sup>[7]</sup> and Matisse.<sup>[9]</sup> In *Still Life with Cabbage* by Ensor [Kröller-Müller Museum (KMM), Otterlo, NL] CdSO<sub>4</sub>·H<sub>2</sub>O and (NH<sub>4</sub>)<sub>2</sub>Cd(SO<sub>4</sub>)<sub>2</sub> white-transparent globules were identified at the paint surface,<sup>[7]</sup> while in *Flowers in a blue vase* by Van Gogh (KMM) amorphous CdSO<sub>4</sub>, CdC<sub>2</sub>O<sub>4</sub> and PbSO<sub>4</sub> were found to be the main constituents of a grayish alteration crust.<sup>[5]</sup> In *Joy of Life* and *Flower Piece* by Matisse (The Barnes Foundation, Philadelphia, USA) the degraded CdY paints are mainly composed of CdSO<sub>4</sub>·nH<sub>2</sub>O, CdC<sub>2</sub>O<sub>4</sub>, CdCO<sub>3</sub> and several cadmium chlorides.<sup>[9]</sup> Cadmium sulfates, being the common constituents of these different alterations, has been interpreted as the direct degradation products of the photo-oxidation of CdS, while the others as the result of its further interaction with the atmosphere or with the paint components.

Nevertheless, limited knowledge of the environmental conditions (e.g., humidity, light, temperature...) in which paintings were stored or displayed over extended period of time and the heterogeneous chemical composition of paint layers (often rendered more complex by later restoration interventions) hamper a thoroughly comprehension of the overall degradation process.

The following key-questions still remain open on CdY alteration: how do environmental conditions (i.e., light and moisture) and the intrinsic properties of CdYs (i.e., composition and crystalline structure) affect their stability and the chemical nature of degradation products? Providing an answer to these questions is highly relevant for understanding the origin and mechanisms of CdYs degradation and for giving predictive indications on their propensity towards deterioration. To this end, the experimental study of mock-up paints before and after artificial aging treatments, aiming at reproducing the alterations encountered in paintings over a shorter time frame, is a valuable strategy.

Here, we present the results obtained from accelerated aging, under controlled conditions of relative humidity (RH) and UVA-Visible light (mimicking museum indoor lighting environments),

[a] Dr. L. Monico, Dr. A. Chieli, Prof. A. Romani, Dr. C. Miliani  
SMAArt Centre and Department of Chemistry, Biology and Biotechnology  
University of Perugia  
Via Elce di Sotto 8, 06123 Perugia, Italy  
and

[b] CNR-Institute of Molecular Science and Technologies (ISTM)  
Via Elce di Sotto 8, 06123 Perugia, Italy  
E-mail: letizia.monico@unipg.it; costanza.miliani@cnr.it

[c] Dr. L. Monico, S. De Meyer, Prof. K. Janssens  
Department of Chemistry  
University of Antwerp  
Groenenborgerlaan 171, 2020 Antwerp, Belgium

[d] Dr. M. Cotte, Dr. W. de Nolf  
ESRF  
Avenue des Martyrs 71, 38000 Grenoble, France

[e] Dr. M. Cotte  
Laboratoire d'Archéologie Moléculaire et Structurale (LAMS),  
Sorbonne Universités, CNRS, UMR 8220  
place Jussieu 4, 75005 Paris, France

[f] Dr. G. Falkenberg  
DESY  
Notkestraße 85, 22607 Hamburg, Germany  
Supporting information for this article is given via a link at the end of the document.

of a series of laboratory-prepared oil mock-up paints made of CdY powders of different stoichiometry (CdS,  $\text{Cd}_{1-x}\text{Zn}_x\text{S}$ ) and crystalline structure (hexagonal, cubic).









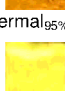
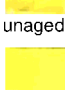
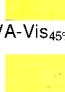
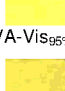
A combination of SR-based X-ray spectromicroscopic methods with macro (MA)-FTIR [both in attenuated total reflection (ATR) and reflection mode] and diffuse reflectance UV-Visible spectroscopies permitted us to perform an in depth characterization of the optical and molecular modifications induced by the aging processes down to the micro-scale length.

## Results and Discussion

### Discoloration response and molecular transformations

Table 1 shows the photographs and summarizes the results of laboratory-prepared oil paints made of hexagonal CdS (hex-CdS), cubic CdS (cub-CdS), or hexagonal  $\text{Cd}_{0.76}\text{Zn}_{0.24}\text{S}$  ( $\text{Cd}_{0.76}\text{Zn}_{0.24}\text{S}$ ) before and after exposure to UVA-Visible light at 45% RH (UVA-Vis<sub>45%RH</sub>) or 95% RH (UVA-Vis<sub>95%RH</sub>) and thermal aging (thermal<sub>95%RH</sub>) (see Experimental Section below for details).

Table 1. Photographs and summary of colorimetric, MA-FTIR, SR  $\mu$ -XRD and S/Cd-speciation results obtained from CdS-based mock-up paints before and after different aging conditions [see Experimental Section and Figures 1-3 and S1-S4 (Supporting Information) for details].

Sample/aging protocol <sup>[a]</sup>	Color change <sup>[b],[c]</sup>	MA-FTIR (ATR-mode)	SR $\mu$ -XRD	S-speciation (SR $\mu$ -XRF, $\mu$ -XANES) $[\text{S}^{\text{VI}}]/[\text{S}^{\text{total}}](\%)$	Cd-speciation (SR $\mu$ -XRF, $\mu$ -XANES)
hex-CdS	 unaged	Lipidic material (oil)	hex-CdS <sup>[e],[f]</sup>	0	CdS-based compound <sup>[g]</sup>
	 UVA-Vis <sub>45%RH</sub>	Oxidation products of the oil	As unaged sample <sup>[e],[f]</sup>	0	As unaged sample
	 UVA-Vis <sub>95%RH</sub>	$\text{CdSO}_4/\text{CdSO}_4 \cdot n\text{H}_2\text{O}$ ; organo-Cd compound(s)	As unaged sample <sup>[e]</sup>	$\approx 10$ (upper 2-3 $\mu\text{m}$ )	As unaged sample
	 thermal <sub>95%RH</sub>	Cd-oxalate; <sup>[d]</sup> oxidation products of the oil	As unaged sample <sup>[e],[f]</sup>	0	As unaged sample
cub-CdS	 unaged	Lipidic material (oil)	cub-CdS <sup>[f]</sup>	0	CdS-based compound <sup>[g]</sup>
	 UVA-Vis <sub>45%RH</sub>	Oxidation products of the oil	As unaged sample <sup>[f]</sup>	0	As unaged sample
	 UVA-Vis <sub>95%RH</sub>	$\text{CdSO}_4/\text{CdSO}_4 \cdot n\text{H}_2\text{O}$ ; organo-Cd compound(s)	As unaged sample <sup>[e]</sup>	$\approx 5-7$ (upper 2-3 $\mu\text{m}$ )	As unaged sample
	 thermal <sub>95%RH</sub>	Cd-oxalate; <sup>[d]</sup> oxidation products of the oil	As unaged sample <sup>[f]</sup>	0	As unaged sample
$\text{Cd}_{0.76}\text{Zn}_{0.24}\text{S}$	 unaged	Lipidic material (oil)	$\text{Cd}_{0.76}\text{Zn}_{0.24}\text{S}$ ; $\text{BaSO}_4$ <sup>[e]</sup>	0; $\text{BaSO}_4$ particles	CdS-based compound <sup>[g]</sup>
	 UVA-Vis <sub>45%RH</sub>	Oxidation products of the oil	As unaged sample <sup>[e]</sup>	As unaged sample	As unaged sample
	 UVA-Vis <sub>95%RH</sub>	$\text{CdSO}_4/\text{CdSO}_4 \cdot n\text{H}_2\text{O}$ ; $\text{ZnCd}_2\text{O}_4 \cdot 2\text{H}_2\text{O}$	$\text{CdSO}_4 \cdot \text{H}_2\text{O}$ ; $\text{ZnCd}_2\text{O}_4 \cdot 2\text{H}_2\text{O}$ ; $\text{BaSO}_4$ <sup>[e]</sup>	$\approx 10-30$ (highest amount within the upper 10 $\mu\text{m}$ )	$\text{CdSO}_4 \cdot \text{H}_2\text{O}$ ( $\approx 40-50\%$ ) and Cd-oxalate within the upper 10 $\mu\text{m}$ ; mainly CdS (down to $\approx 90\%$ ) in the middle-bottom yellow paint.
	 thermal <sub>95%RH</sub>	Zn-carboxylates; oxidation products of the oil	As unaged sample <sup>[e]</sup>	As unaged sample	As unaged sample

[a] See ref.<sup>[3]</sup> for the optical, molecular spectroscopic and crystalline structure results of the powder. [b] See Figure S1 for the diffuse reflectance UV-Vis spectra of the unaged and UVA-Vis light aged samples. [c] The calculated band gap energies ( $E_g$ ) are: 2.43 eV for hex-CdS, 2.35 eV for cub-CdS and 2.65 eV for  $\text{Cd}_{0.76}\text{Zn}_{0.24}\text{S}$  (see Supporting Information for further details). The values are comparable before and after aging. [d] Revealed only by reflection mode MA-FTIR analysis (Figure S3). Mapping measurements performed on thin sections in transmission mode at: [e] P06-DESY beamline; [f] ID21-ESRF beamline (results not shown). [g] The Cd L<sub>3</sub>-edge XANES spectra of hex-CdS, cub-CdS and  $\text{Cd}_{0.76}\text{Zn}_{0.24}\text{S}$  are very similar.

In order to assess the chromatic and molecular changes promoted by different ageing procedures at the paint surface, first UV-Vis/colorimetric investigations of the photochemically aged samples were performed, followed by FTIR spectroscopic analyses of all mock-ups.

Colorimetric measurements (Table 1) allowed to observe that the total color change ( $\Delta E^*$ ) is slightly perceptible at the naked eye ( $<3$ ) for UVA-Vis<sub>45%RH</sub> paints, while it becomes appreciable after UVA-Vis<sub>95%RH</sub> aging, achieving values of 15, 12 and 9 for hex-CdS, cub-CdS and Cd<sub>0.76</sub>Zn<sub>0.24</sub>S, respectively. The corresponding diffuse reflectance UV-Vis spectral modifications (Figure S1: red lines, Supporting Information) show a red shift of the absorption spectrum as the main modification, leading to an increase in yellowness ( $\Delta b^*$ : from 8 to 12), which corresponds to the major contribution to  $\Delta E^*$ , whereas variations in lightness ( $\Delta L^*$ : 2-3) and redness ( $\Delta a^*$ : from -2 to -4) are smaller (Table 1).

The ATR mode FTIR spectra recorded from the three UVA-Vis aged samples at 45% RH (Figure 1: blue lines, compared to the unaged samples, black lines) show the broadening and slight wavenumber shifts of the CH stretching [ $\nu(\text{CH})$ ] and CO ester asymmetric stretching [ $\nu(\text{CO})$ ] modes of the triglycerides, along with the intensity increase of the band at 1620-1635  $\text{cm}^{-1}$ . These changes resemble the ones observed in the unpigmented linseed oil [14] and are attributable to the formation of different secondary compounds with low molecular weight (e.g., alcohols, ketones, aldehydes, carboxylic acids...) due to the oxidation of the oil.

Similar spectral variations are also observable in the FTIR spectra of hex-CdS and cub-CdS paints after UVA-Vis aging at 95% RH (Figure 1: red lines), but they occur along with the presence of new signals in the 1000-1200  $\text{cm}^{-1}$  range and below 650  $\text{cm}^{-1}$ , both ascribable to CdSO<sub>4</sub> [ $\nu_{1/3}(\text{SO}_4^{2-})$  and  $\nu_4(\text{SO}_4^{2-})$ , respectively] (Figure S2, Supporting Information). Two additional broad bands at around 1560-1545  $\text{cm}^{-1}$  and 1410-1405  $\text{cm}^{-1}$  are also visible, probably related to Cd-organo compounds (Figure S2). The UVA-Vis<sub>95%RH</sub> aging of Cd<sub>0.76</sub>Zn<sub>0.24</sub>S led, next to CdSO<sub>4</sub>, also to the formation of ZnC<sub>2</sub>O<sub>4</sub>·2H<sub>2</sub>O, whose presence is pointed out by the IR bands at 1640, 1364, 1317, 818  $\text{cm}^{-1}$  (Figures 1 and S2). This compound is likely the result of the reaction between Zn<sup>2+</sup> ions of the pigment and the oxalate ions arising from the oil oxidation.[15] The strong intensity decrease of  $\nu(\text{CH})$  modes and disappearance of  $\nu(\text{CO})$  band of triglycerides, more pronounced than that observed for hex-CdS and cub-CdS paints subject to the same aging conditions, suggests the almost complete oxidative degradation of the binder. The phenomenon manifests itself as visible chalking and gloss decrease of the paint surface, similar to the earlier observations by Leone et al. on aged commercial and historical CdS-based pigments.[13]

It is noteworthy that the formation of cadmium sulfates is detectable by FTIR only after the UVA-Vis<sub>95%RH</sub> treatment.

ATR mode FTIR spectra acquired from the three thermally aged samples (RH=95%, T=40°C) (Figure 1: grey lines) show the disappearance of  $\nu(\text{CO})$  band of esters at ~1735  $\text{cm}^{-1}$  and the increase of  $\nu(\text{CO})$  band of free fatty acids at 1715-1705  $\text{cm}^{-1}$ , suggesting that, as expected,[16] humidity and temperature promoted the hydrolysis of triglycerides. Through the reaction with Zn<sup>2+</sup> cations released by Cd<sub>0.76</sub>Zn<sub>0.24</sub>S, the free fatty acids

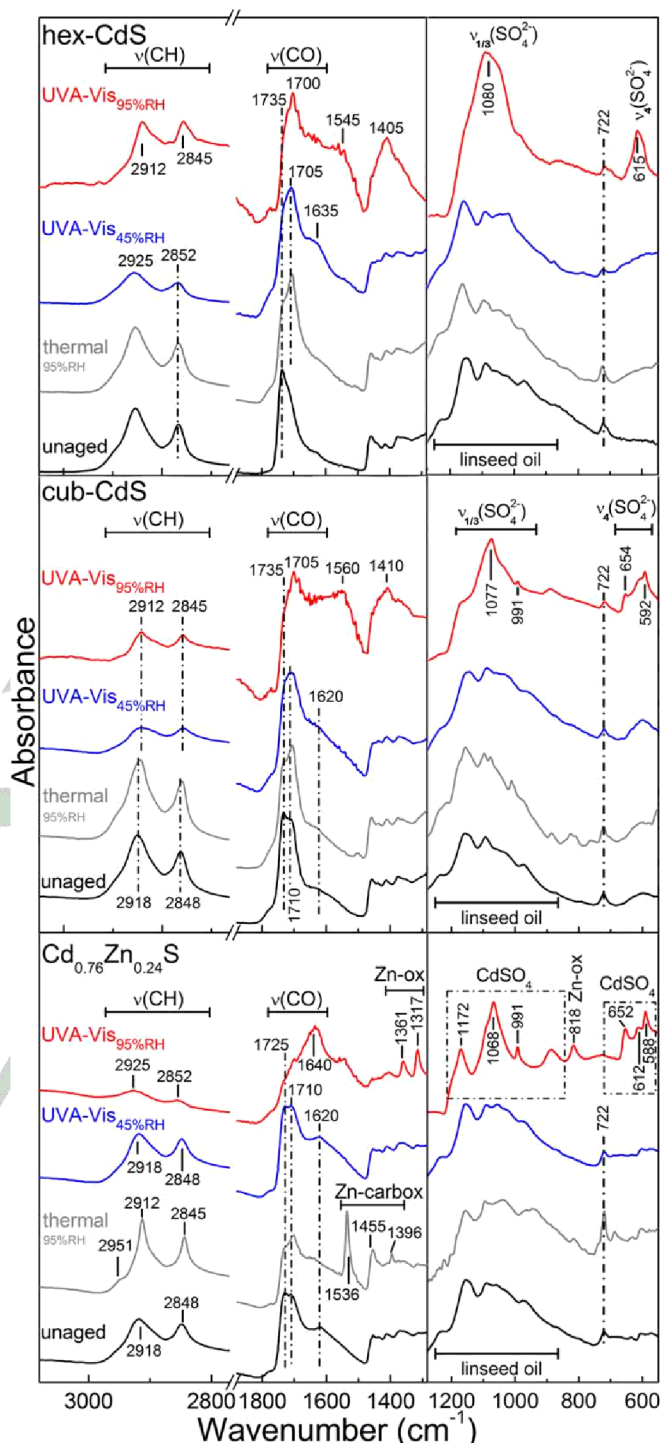


**Figure 1.** ATR-FTIR spectra of (from top to bottom) hex-CdS, cub-CdS and Cd<sub>0.76</sub>Zn<sub>0.24</sub>S paints before (black) and after UVA-Vis light exposure at 45% RH (blue) or 95% RH (red) and thermal aging (grey) (see Table 1 for details and Figures S2-S3 for the spectra of reference compounds and a selection of the corresponding reflection mode FTIR profiles).

gave rise to the formation of Zn-carboxylates (also known as Zn-soaps) at the paint surface with IR bands at 1536, 1455 and 1396  $\text{cm}^{-1}$  that are similar to those of zinc stearate and/or palmitate (Figure S2). The significantly lower solubility of Zn-carboxylates compared to that of Cd-carboxylates[18] may

provide an explanation of why the employed aging conditions have favored the formation of the former compounds. Zn-carboxylates have often been identified in oil paintings,<sup>[10a,12a,15,17]</sup> with consequent negative effects on both the mechanical and aesthetical properties of the artworks. In hex-CdS/thermal<sub>95%RH</sub> and cub-CdS/thermal<sub>95%RH</sub> paints, the sensitivity of reflection mode MA-FTIR spectroscopy to surface components,<sup>[19]</sup> permitted us to reveal the presence of  $\text{CdC}_2\text{O}_4 \cdot 3\text{H}_2\text{O}$  as a degradation product (weak derivative-like bands at 1310 and 785  $\text{cm}^{-1}$ ; Figure S3, Supporting Information).

#### Sulfur and cadmium speciation investigations and $\mu$ -XRD analysis

To gain insights into the distribution and chemical nature of different S- and Cd-compounds at the micrometric scale, in a second phase of this investigation, we have analyzed all unaged and aged CdY-based paints as thin sections by SR-based  $\mu$ -XRF chemical state mapping, S K-edge and Cd L<sub>3</sub>-edge  $\mu$ -XANES spectroscopy and by SR-based  $\mu$ -XRD mapping (Figures 2 and 3).

The results arising from the thermal<sub>95%RH</sub> and UVA-Vis<sub>45%RH</sub> aged samples are similar to those obtained from the equivalent unaged paints, confirming the FTIR-based observation that the conversion from sulfides to sulfates does not take place as a consequence of these treatments. In Figure S4 (Supporting Information) a selection of the S K-edge  $\mu$ -XANES spectra and S chemical state maps obtained from the thermal<sub>95%RH</sub> aged paints is shown. The S chemical state maps collected from UVA-Vis<sub>95%RH</sub> samples (Figures 2B,E and 3D) reveal that the aging gave rise to the formation of a thin S<sup>VI</sup>-rich layer (2-10  $\mu\text{m}$  in thickness) at the paint surface, whereas S<sup>II</sup>-species are the main constituents of the paint underneath. One-dimensional series of S K-edge XANES spectra collected from each sample vs. depth below the exposed surface are shown in Figures 2C, F and 3E (only a selection of the acquired spectra is reported), demonstrating that the typical feature of S<sup>VI</sup>-based compounds (2.482 keV)<sup>[20]</sup> is appreciable only in the profiles acquired from the top surface of aged hex-/cub-CdS paints and it is more pronounced in those recorded within the upper 9-10  $\mu\text{m}$  of the aged  $\text{Cd}_{0.76}\text{Zn}_{0.24}\text{S}$  paint. To determine quantitatively the average relative amount of S<sup>VI</sup>- and S<sup>II</sup>-species (expressed as  $\%[\text{S}^{\text{VI}}]/[\text{S}_{\text{total}}]$  and  $\%[\text{S}^{\text{II}}]/[\text{S}_{\text{total}}]$ ), we have described each XANES spectra as a linear combination fit (LCF) of a set of S-reference compounds [see Table S1 (Supporting Information) for details about the fit results]. Three fitting components, i.e. (i)  $\text{Cd}_{0.76}\text{Zn}_{0.24}\text{S}$ , (ii)  $\text{CdSO}_4 \cdot n\text{H}_2\text{O}$  (with  $n$  either equal to 0, 1 or 8/3) and (iii)  $\text{BaSO}_4$  (already originally present as an additive of the pigment's formulation and distributed in the forms of minute particles within the paint; see Table 1 and Figure S4B), were necessary to obtain a good description of the spectra recorded along the line obtained from  $\text{Cd}_{0.76}\text{Zn}_{0.24}\text{S}$ . The spectra acquired from hex-/cub-CdS could be properly fitted using just 2 components (either CdS or  $\text{Cd}_{0.76}\text{Zn}_{0.24}\text{S}$  in addition to  $\text{CdSO}_4 \cdot n\text{H}_2\text{O}$ ). Within the first upper micrometer of the hex-CdS and cub-CdS paints, the average amount of oxidized S<sup>VI</sup> was estimated to be around 10% and 6%, respectively (Table S1), while it reaches ca. 20-25% in the upper 9  $\mu\text{m}$  of  $\text{Cd}_{0.76}\text{Zn}_{0.24}\text{S}$ .

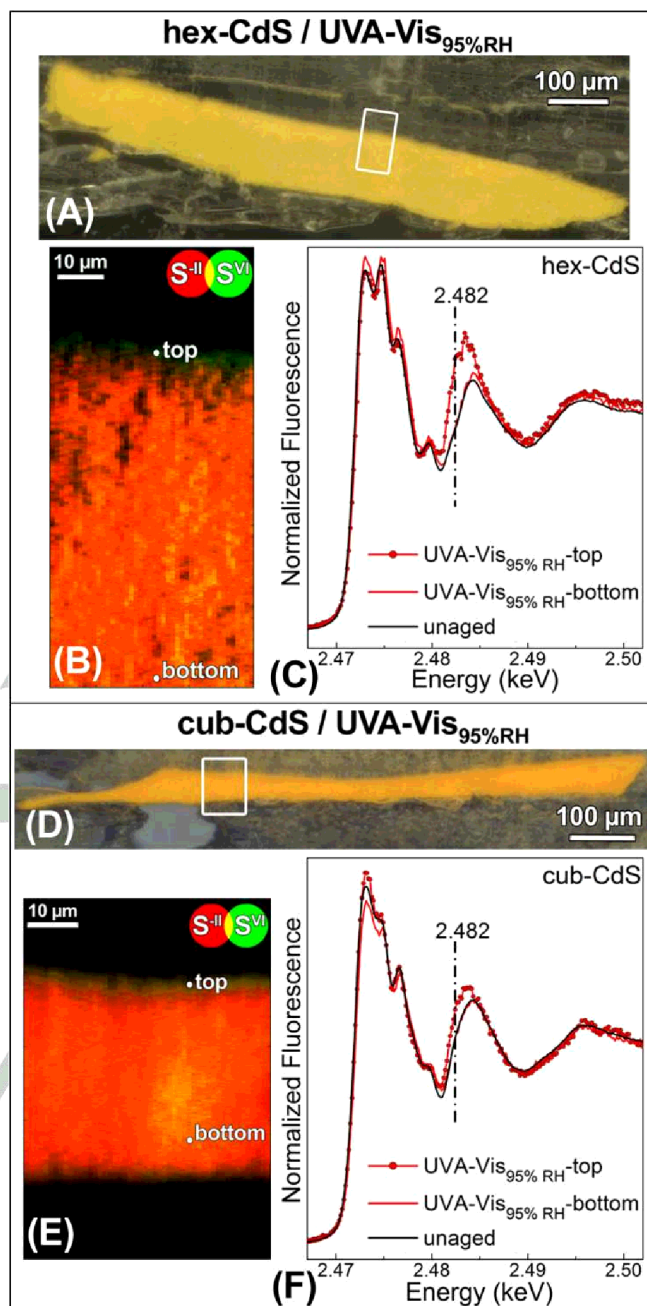


**Figure 2.** Photomicrographs of (A) hex-CdS and (D) cub-CdS thin sections after UVA-Vis light exposure at 95% RH. (B, E) RG composite SR  $\mu$ -XRF maps of S<sup>II</sup>/S<sup>VI</sup> [step size (h×v): 1×0.3  $\mu\text{m}^2$ , exp. time: 100 ms/pixel, energy: 2.473-3.7 keV] acquired in the region shown by the white rectangle in (A, D). (C) Selection of S K-edge  $\mu$ -XANES spectra (red) obtained from the areas reported in (B,E). In black, spectrum recorded from the surface of the equivalent unaged material (see Table S1 for details about the LCF results).

(Figure 3E: left-side panel; Table S1). For the latter, the abundance of S<sup>VI</sup> progressively decreases with increasing depth down to values of about 7% where it is likely mainly due to  $\text{BaSO}_4$ . Only S<sup>II</sup>-species could be detected at the bottom surface (neither exposed to light nor to humidity) of hex-CdS and cub-CdS paints, the XANES spectra strongly resembling those of the corresponding unaged paint (i.e., only CdS).

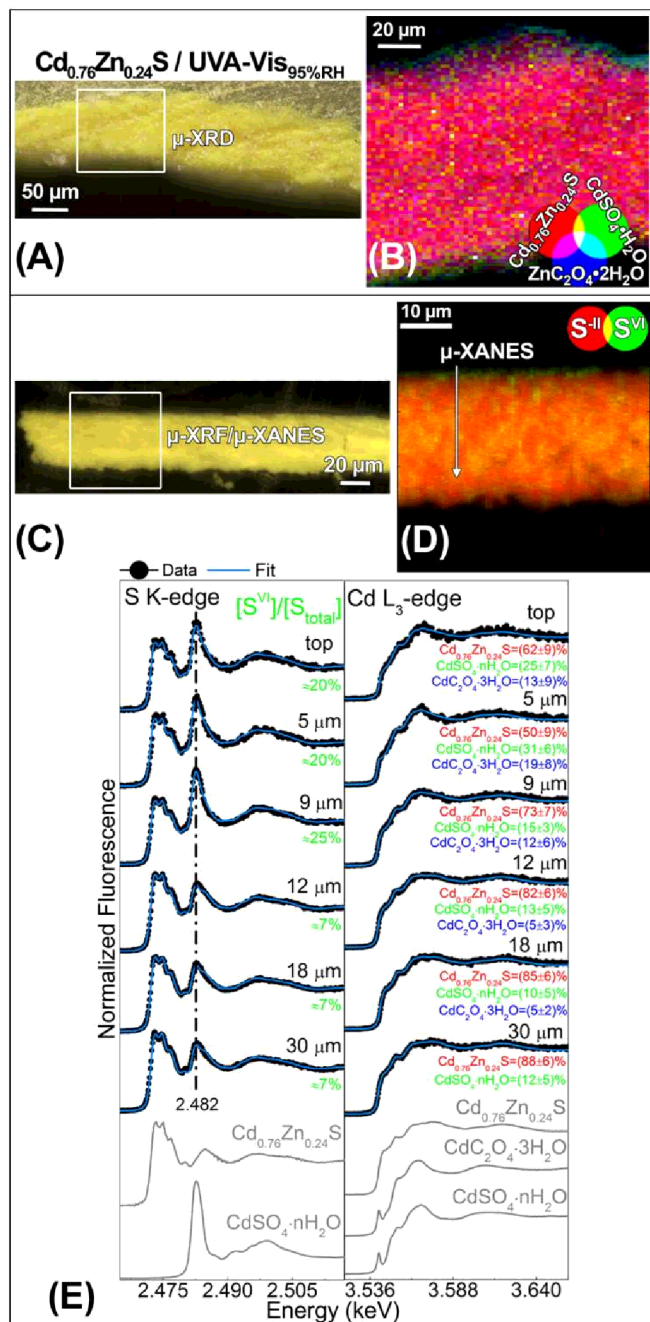


**Figure 3.** (A,C) Photomicrograph of two  $\text{Cd}_{0.76}\text{Zn}_{0.24}\text{S}$  thin sections after UVA-Vis light exposure at 95% RH. RGB composite (B) SR  $\mu$ -XRD maps of  $\text{Cd}_{0.76}\text{Zn}_{0.24}\text{S}$ / $\text{CdSO}_4 \cdot \text{nH}_2\text{O}$ / $\text{ZnC}_2\text{O}_4 \cdot 2\text{H}_2\text{O}$  [step size (h×v):  $2 \times 1.5 \mu\text{m}^2$ , exp. time: 1 s/pixel, energy: 21 keV] and (D) SR  $\mu$ -XRF maps of  $\text{S}^{\text{II}}$ / $\text{S}^{\text{VI}}$  [step size (h×v):  $1 \times 0.3 \mu\text{m}^2$ , exp. time: 100 ms/pixel, energy: 2.473–3.7 keV] recorded from the region shown by the white rectangle in (A,C). (E) Selection of S K-edge and Cd L<sub>3</sub>-edge  $\mu$ -XANES spectra obtained from the arrow shown in (D) (see Table S1 for detail about the LCF results).

Cd L<sub>3</sub>-edge  $\mu$ -XANES spectra recorded from the top and bottom sides of hex-CdS and cub-CdS samples are similar, due to the dominance of CdS spectral features (results not reported). Similar analysis performed on  $\text{Cd}_{0.76}\text{Zn}_{0.24}\text{S}$  permitted us to complement the S K-edge investigations (Figure 3E: right-side panel). Notably, the LCF results reveal that within the uppermost 9 μm of the paint,  $\text{CdSO}_4 \cdot \text{nH}_2\text{O}$  (~25–30%) and  $\text{Cd}_{0.76}\text{Zn}_{0.24}\text{S}$

(~50–60%) are likely present together with a third component, such as  $\text{CdC}_2\text{O}_4 \cdot 3\text{H}_2\text{O}$ . Its content progressively disappears with increasing of depth values, while that of  $\text{CdSO}_4 \cdot \text{nH}_2\text{O}$  decreases down to a relative abundance at around 12%. SR-based  $\mu$ -XRD mapping analyses acquired from  $\text{Cd}_{0.76}\text{Zn}_{0.24}\text{S}$ /UVA-Vis<sub>95%RH</sub> (Figure 3A,B) are in line with the FTIR and  $\mu$ -XRF/μ-XANES results (Figures 1 and 3D,E), revealing the formation of a layer composed of  $\text{CdSO}_4 \cdot \text{nH}_2\text{O}$  and  $\text{ZnC}_2\text{O}_4 \cdot 2\text{H}_2\text{O}$  (thickness ~5 μm) at the paint surface as the result of the aging process.  $\mu$ -XRD measurements of hex-CdS and cub-CdS paints after UVA-Vis<sub>95%RH</sub> aging (results not shown) did not detect any secondary compounds (i.e.,  $\text{CdSO}_4$ , organo Cd-compounds), likely due to their amorphous nature.

#### Photo-oxidation mechanism of CdS-based pigments in the oil binder under UVA-Vis light and different moisture conditions

Within the boundaries of the employed experimental conditions, our results have established that the photo-oxidation of CdS-based pigments to  $\text{CdSO}_4$ / $\text{CdSO}_4 \cdot \text{nH}_2\text{O}$  in the oil binder requires the presence of humidity. The process (also known as photodissolution or photocorrosion) occurs along with the formation of Zn-oxalate and Cd-organo compounds, proving the potential of CdS-based particles to act as photocatalysts for the oil oxidation.

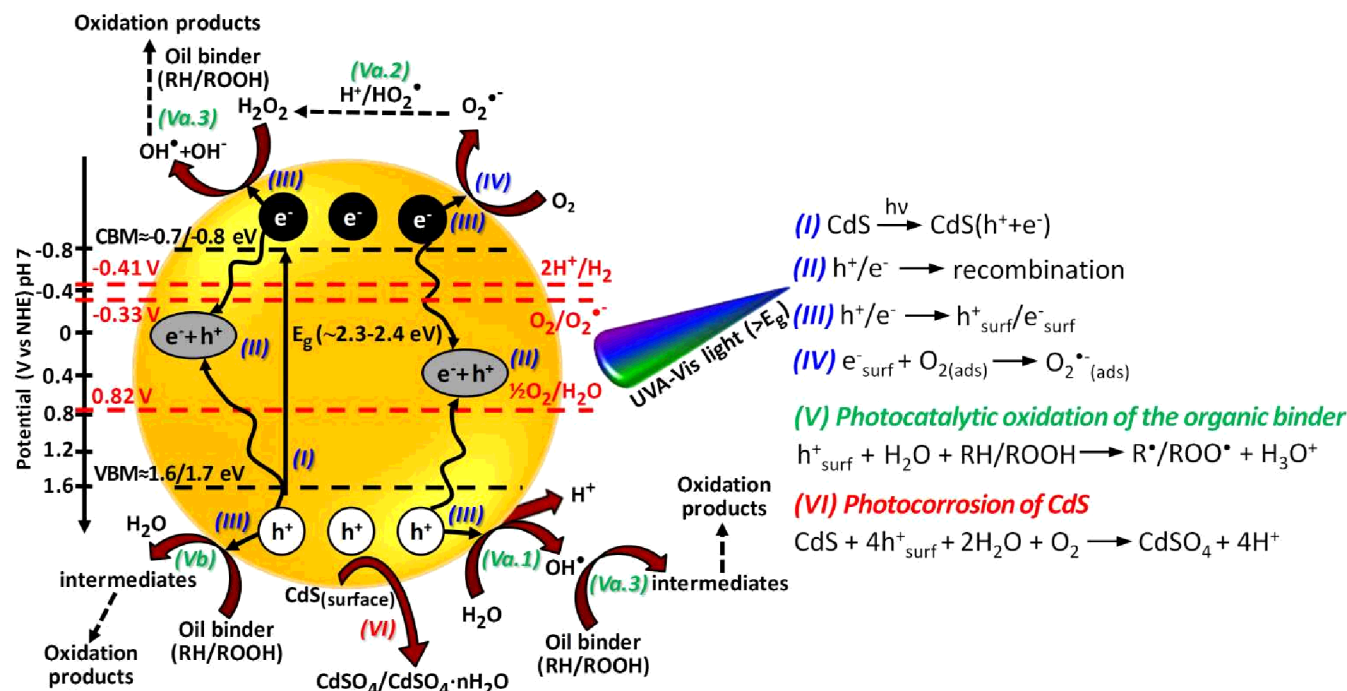
Based on the experimental evidence discussed above and earlier studies about photocatalysis<sup>[21–24]</sup> and photocorrosion<sup>[25–29]</sup> processes of CdS, we propose the mechanism for the photo-oxidation of CdY oil paints under variable moisture conditions shown in Scheme 1.

For explaining the photochemical reactivity of CdS in the oil binder, the energies of the valence band maximum (VBM) and conduction band minimum (CBM) are compared with the thermodynamic redox potential ( $\Phi$ ) of the semiconductor and of water relative to NHE (normal hydrogen electrode) at pH 7. Although these values are pH dependent,<sup>[30]</sup> we can consider them to be reliable since in oil paintings the chemical environment is neutral/slightly acid.<sup>[31]</sup>

Upon illumination with supra-band gap light ( $h\nu > E_g$ ), CdS-based pigment generates electron–hole ( $e^-h^+$ ) pairs (step I) which can either recombine (step II), dissipating the absorbed light energy as heat or radiation, with no chemical effect, or migrate to the surface of particles (step III).

Since the CBM of CdS (~0.7/0.8 eV) is more negative than the redox potential  $\Phi(\text{O}_2/\text{O}_2^{\cdot-}) = -0.033 \text{ eV}$ ,<sup>[23,32,33]</sup> the photogenerated electrons can transfer to  $\text{O}_{2(\text{ads})}$  (adsorbed at the particle surface) and form  $\text{O}_2^{\cdot-}(\text{ads})$  (step IV).

The photocatalytic oxidation of the organic binder may either take place *via* interaction with hydroxyl radicals ( $\text{OH}^{\cdot}$ ) (path a: steps Va.1–3) and/or photogenerated  $h^+$  (path b: step Vb) [see Scheme S1 (Supporting Information) for the complete sequence of chemical reactions]. In aqueous systems, it has been observed that the former process is favoured at pH greater than 6, while the latter becomes dominant at pH values below 6.<sup>[34]</sup> Consistent with literature reports,<sup>[22,23]</sup>  $\text{OH}^{\cdot}$  species may be generated through the reaction between surface-adsorbed  $\text{H}_2\text{O}$  ( $\text{OH}^-$ ) and photogenerated  $h^+$  (step Va.1). The process is thermodynamically possible because surface-



**Scheme 1.** Proposed mechanism for the photocorrosion of CdS-based pigments and photocatalytic oxidation process of the oil binder over CdS-based particles [see Scheme S1 (Supporting Information) for the complete sequence of chemical reactions].

adsorbed OH<sup>-</sup> groups may be oxidized to OH<sup>•</sup> radicals at a lower redox potential [ $\phi(\text{OH}^{\bullet}_{(\text{ads})}/\text{OH}^{\bullet}_{(\text{ads})}) \approx 1.5 \text{ V}$ ] than free OH<sup>-</sup> groups [ $\phi(\text{OH}^{\bullet}_{(\text{free})}/\text{OH}^{\bullet}_{(\text{free})}) = 2.3\text{--}2.4 \text{ V}$ ], which is indeed more negative than VBM of CdS ( $\sim 1.6\text{--}1.7 \text{ eV}$ ).<sup>[23,35]</sup> Alternatively OH<sup>-</sup> can be produced via the reduction pathway of H<sub>2</sub>O<sub>2</sub> (step Va.2), which formation starts with the interaction of O<sub>2</sub><sup>-</sup><sub>(ads)</sub> with H<sup>+</sup><sub>(ads)</sub>.<sup>[22,28]</sup> The generated OH<sup>•</sup> radical reacts then with the binding medium to form a R<sup>•</sup>/ROO<sup>•</sup> species by the abstraction of H<sup>•</sup> (step Va.3) and are ultimately transformed to oxidized organo-Cd/Zn compounds (Figures 1 and 3B). Simultaneously, h<sup>+</sup> can react directly with the surface-adsorbed lipids to form oxidized species by releasing H<sup>•</sup>/H<sup>•</sup> and R<sup>•</sup>/ROO<sup>•</sup> as intermediates of the photocatalytic oxidation process of the oil (step Vb).<sup>[21,27,36]</sup> The CdS dissolution/corrosion (step VI) is a process that may compete with the photocatalytic oxidation of the oil by depleting photogenerated h<sup>+</sup>.<sup>[27,34]</sup> It has been reported that a semiconductor is stable with respect to h<sup>+</sup> oxidation if its thermodynamic oxidation potential ( $\phi^{\text{ox}}$ ) and its VBM are both lower than  $\phi(\text{O}_2/\text{H}_2\text{O})$  (0.82 V).<sup>[30]</sup> These conditions are not satisfied for CdS-pigments since its  $\phi^{\text{ox}}$  ( $\sim 0.3\text{--}0.5 \text{ V}$ )<sup>[32,37]</sup> is lower than  $\phi(\text{O}_2/\text{H}_2\text{O})$  and its VBM is higher than  $\phi(\text{O}_2/\text{H}_2\text{O})$ . The only possibility for CdS to undergo photocorrosion is then through the interaction between the photogenerated h<sup>+</sup> and adsorbed SH<sup>-</sup> (step VI; see also Scheme S1 for further details).<sup>[25–28]</sup> This process may give rise to SH<sup>•</sup> species, that, in the presence of O<sub>2</sub> and H<sub>2</sub>O, can be finally transformed into cadmium sulfate (Scheme 1 and Figures 1–3).<sup>[21,25–29]</sup> Although we found no evidence of the presence of any S-species of oxidation between -II and +VI, it has been described that the photo-corrosion process of CdS may proceed via various S<sup>IV</sup>-species intermediates such as SO<sub>2</sub><sup>-</sup>, HSO<sub>3</sub><sup>-</sup>/SO<sub>3</sub><sup>2-</sup> (Scheme S1).<sup>[25–28]</sup>

We observed that, upon exposure to light and moisture (95% RH), Cd<sub>0.76</sub>Zn<sub>0.24</sub>S shows a higher tendency towards photocorrosion than hex-CdS and cub-CdS, as pointed out by an increased relative amount of CdSO<sub>4</sub>·H<sub>2</sub>O formed (Figures 2–3 and Table S1). It is known that the valence band width of a semiconductor controls the mobility of photogenerated h<sup>+</sup>.<sup>[38]</sup> Thus, the wider the valence band width, the higher the mobility of h<sup>+</sup>, and the better the photo-oxidation efficacy of h<sup>+</sup>. Since Cd<sub>1-x</sub>Zn<sub>x</sub>S solid solutions have a wider valence band width than that of CdS,<sup>[39]</sup> this may explain why the photo-corrosion of Cd<sub>0.76</sub>Zn<sub>0.24</sub>S is more severe than that of hex-/cub-CdS.

Upon high moisture conditions, we have also demonstrated that Cd<sub>0.76</sub>Zn<sub>0.24</sub>S is a more efficient photocatalyst for the oxidation of adjacent organic material than hex-CdS and cub-CdS (Figure 1), as proved by the almost complete disappearance of the original oil binder at the paint surface and the formation of ZnC<sub>2</sub>O<sub>4</sub>·2H<sub>2</sub>O. The band gap energy ( $E_g$ ) progressively increases for cub-CdS (2.35 eV), hex-CdS (2.43 eV) and Cd<sub>0.76</sub>Zn<sub>0.24</sub>S (2.65 eV) (Table 1, footnote [b]), with the result that, compared to cub-CdS and hex-CdS, the relative positions of CBM and VBM of Cd<sub>0.76</sub>Zn<sub>0.24</sub>S are shifted toward more negative and positive potential values respectively.<sup>[40a]</sup> Elevation of the CBM with respect to the water reduction level [ $\phi(2\text{H}^+/\text{H}_2) \approx -0.41 \text{ V}$ ] increases the thermodynamic drive force for water reduction,<sup>[39,40]</sup> thus improving the photocatalytic activity of Cd<sub>0.76</sub>Zn<sub>0.24</sub>S for the oil oxidation.

Earlier literature about CdS-based photocatalysts,<sup>[21]</sup> and TiO<sub>2</sub>-pigmented paints<sup>[41]</sup> reports that the photocorrosion and

photocatalytic activity of the semiconductors goes up with increasing humidity levels. This is in line with the results of our study, which showed that the photocatalytic activity and photo-

corrosion of CdS-based pigments occur only upon exposure to light at 95% RH. The higher permeability through pigmented-binders of water than that of  $O_2$ <sup>[41a]</sup> and its absorption on semiconductor surface can play a key role in favoring the formation and stabilization of radicals during the oxidation reaction stages,<sup>[21,22]</sup> thus diminishing the probability for  $h^+/e^-$  recombination (step II). The latter process can be considered the most favored one when the CdS-paints are photochemically aged at environmental humidity levels (45% RH), providing a reasonable explanation for the observed stability of the pigment towards photo-oxidation and its inefficiency as a photocatalyst upon light exposure upon lower humidity conditions.

## Conclusions

In this work, we have identified the main factors driving the degradation of various CdS-based yellows in the oil binder and elucidated how they affect the overall process by combining SR-based X-ray techniques with diffuse reflectance UV-visible and FTIR spectroscopies. Within the boundaries of our experimental conditions, the study of artificially aged mock-up paints led us to draw the following conclusions, which namely represent the answers to the starting questions proposed in the introduction of this study:

(i) the photocorrosion of yellow  $CdS/Cd_{0.76}Zn_{0.24}S$  to white  $CdSO_4/CdSO_4 \cdot nH_2O$  and their photocatalytic activity are triggered by moisture, taking place at ~95% RH but not at "regular" environmental humidity (~45% RH). With decreasing moisture levels electron-hole recombination becomes dominant, thus hindering the photo-oxidation processes in cadmium yellow paints.

(ii) The stability of CdS-based yellows and the chemical nature of the corresponding alteration products depends both on the Cd/Zn stoichiometry and employed aging conditions but not on the crystalline structure of the pigment.  $Cd_{0.76}Zn_{0.24}S$  undergoes photodegradation more readily than CdS and it is a more efficient photocatalyst for the oil oxidation. The inclusion of Zn in the CdS structure widens the valence bandwidth and raises the conduction band minimum. The former is responsible for the enhanced photocorrosion of  $Cd_{0.76}Zn_{0.24}S$ , while the latter improves its photocatalytic activity. Upon light exposure at 95% RH, the formation of a superficial  $CdSO_4/CdSO_4 \cdot H_2O$  layer (~2-10  $\mu m$  thickness) occurred along with the photocatalytic oil oxidation, which gives rise to either organo Cd-compounds (for CdS) or Zn-oxalate (for  $Cd_{0.76}Zn_{0.24}S$ ). In highly moist, dark conditions (~95% RH), the  $S^{2-} \rightarrow SO_4^{2-}$  conversion is hindered and either Cd-oxalates (for CdS) or Zn-carboxylates (for  $Cd_{0.76}Zn_{0.24}S$ ) could be observed as result of the interaction between the pigment and the oxidation products of the oil.

Our findings have important implications for the conservation practice and diagnostic investigations of oil paintings. The photo-oxidation of CdS-based yellow paints may be mitigated by minimizing their exposure to excessively high moisture levels (i.e., <50% RH). We suggest that both Zn-oxalate and Zn-carboxylates might be used as diagnostic markers for the assessment of the state of degradation of  $Cd_{1-x}Zn_xS$  paints, these being the compounds identified in  $Cd_{1-x}Zn_xS$  areas of masterpieces by G. Dottori,<sup>[15]</sup> P. Mondrian<sup>[10a]</sup> and J. Pollock.<sup>[12a]</sup> Nevertheless, care should be taken when the CdS-pigment is

mixed with zinc white (ZnO) to avoid misleading/partial conclusions, due to the well-known tendency of ZnO towards the formation of zinc carboxylates/zinc oxalates as well.<sup>[15-17]</sup>

Questions remain open about what the effects of Cl-compounds and other additives/residual of the synthesis of CdS-based pigments are on the oxidation of CdY paints of *the Scream* by Munch<sup>[8]</sup> and *Joy of Life* by Matisse.<sup>[9]</sup> Thus, further research is ongoing for systematically investigating also these aspects.

## Experimental Section

### Preparation of CdS-based mock-up paints and accelerated aging experiments

Mock-up paints were prepared by mixing commercial powders of hexagonal CdS (Sigma Aldrich), cubic CdS (in-house synthesized) or hexagonal  $Cd_{0.76}Zn_{0.24}S$  (Kremer GmbH) with linseed oil (Zecchi) in a 4:1 mass ratio. These mixtures were applied on areas of about  $1.5 \times 1.5 \text{ cm}^2$  to a polycarbonate support. Further information about the synthesis, crystalline structure and optical/molecular properties of hexagonal CdS, cubic CdS, and hexagonal  $Cd_{0.76}Zn_{0.24}S$  (in this work denoted as hex-CdS, cub-CdS and  $Cd_{0.76}Zn_{0.24}S$ ) are reported in a previous study.<sup>[3]</sup>

UVA-Visible photochemical aging treatments were carried out by means of an in-house made aging chamber equipped with a UV-filtered 300 W Cermox xenon lamp ( $\lambda \geq 300 \text{ nm}$ ) (see ref.<sup>[42]</sup> for the corresponding emission spectral profile) either at ~45% RH (measured indoor humidity level) or at ~95% RH. The measured illuminance and temperature at the samples position were  $1 \times 10^5$ - $1.8 \times 10^5 \text{ lux}$  (irradiance:  $1.8 \times 10^5$ - $3.0 \times 10^5 \mu W/cm^2$ ) and 25-30 °C, respectively. Paints were irradiated for 430-640 h such to achieve total luminous exposure values of  $5 \times 10^7$ - $1 \times 10^8 \text{ lux} \cdot h$  (total irradiance:  $9 \times 10^7$ - $1.9 \times 10^8 \mu W/cm^2 \cdot h$ ).

Thermal aging treatments were performed by placing the touch-dried paints (i.e., after about one month since their preparation) in two sealed vessels maintained at different RH conditions: ca. 50% using a  $Mg(NO_3)_2 \cdot 6H_2O$  (Sigma Aldrich) saturated solution and >95% with distilled water. Both vessels were kept in the dark at 40°C for an overall period of about 90-100 days (2160-2400 h). Since similar results were obtained from the aging under 50% and 95% RH conditions only those arising from the latter experiments are shown and described in this work.

### Analytical methods

The surface of paint samples was analyzed before and after different aging treatments by means of the following non-invasive/non-destructive spectroscopic methods: diffuse reflectance UV-Visible and MA-FTIR both in ATR and reflection mode.

Thin sections (2-10  $\mu m$  in thickness) were obtained with a microtome from all unaged/aged samples and analyzed by combining SR-based  $\mu$ -XRF/ $\mu$ -XANES at S K- and Cd  $L_{3-}$ edges (scanning X-ray microscope end-station of beamline ID21 at ESRF, Grenoble)<sup>[43]</sup> and SR-based  $\mu$ -XRD mapping ( $\mu$ -XRD/ $\mu$ -XRF end-station of beamline ID21-ESRF<sup>[43]</sup> and beamline P06-PETRA III at DESY, Hamburg).<sup>[44]</sup>

Additional details about the instruments and the employed experimental conditions are described in the Supporting Information.

## Acknowledgements

The research was financially supported by the European research project IPERION-CH, funded by the European Commission, H2020-INFRAIA-2014-2015 (Grant agreement n. 654028) and by the BOF-GOA Project SOLARPaint (University of Antwerp Research Council).

For the beamtime grants received, we thank the ESRF (experiments n. HG64, HG95 and in-house beamtimes) and PETRA III-DESY (experiments: I-20130221 EC, I-20160126 EC).

We are also grateful to Dr. Jan Garrevoet for its contribution to set up the P06-beamline at PETRA III-DESY.

**Keywords:** photochemistry • photocatalysis • cadmium sulfide • pigments • artworks

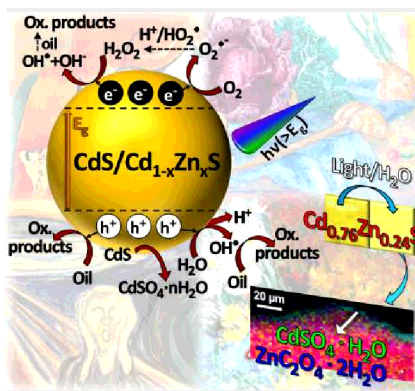
- [1] I. Fiedler and M. Bayard, in *Artist's Pigments, A Handbook of their History and Characteristics*, Vol. 1 (Ed. R. L. Feller), National Gallery of Art, Washington, 1986, pp. 65-108.
- [2] W. G. Huckle, G. F. Swigert, S. E. Wiberley, *Ind. Eng. Chem. Prod. Res. Dev.* **1966**, *5*, 362-366.
- [3] F. Rosi, C. Grazia, F. Gabrieli, A. Romani, M. Paolantoni, R. Vivani, B. G. Brunetti, P. Colombari, C. Miliani, *Microchem. J.* **2016**, *124*, 856-867.
- [4] a) A. Roy, *National Gallery Technical Bulletin* **2007**, *28*, 58-68; b) P. Dredge, R. Wührer, M. R. Phillips, *Microsc. Microanal.* **2003**, *9*, 139-143.
- [5] G. Van der Snickt, K. Janssens, J. Dik, W. De Nolf, F. Vanmeert, J. Jaroszewicz, M. Cotte, G. Falkenberg, L. van der Loeff, *Anal. Chem.* **2012**, *84*, 10221-10228.
- [6] J. Kirby, K. Stonor, A. Roy, A. Burnstock, R. Grout, R. White, *National Gallery Technical Bulletin* **2003**, *24*, 4-37.
- [7] G. Van der Snickt, J. Dik, M. Cotte, K. Janssens, J. Jaroszewicz, W. De Nolf, J. Groenewegen, L. van der Loeff, *Anal. Chem.* **2009**, *7*, 2600-2610.
- [8] a) B. Singer, T. E. Aslaksby, B. Topalova-Casadio, E. S. Tveit, *Stud. Conserv.* **2010**, *55*, 274-292; b) *Public Paintings by Edvard Munch and His Contemporaries: Change and Conservation Challenges* (Eds. T. Frøysaker, N. Streeton, H. Kutzke, F. Hanssen-Bauer, B. Topalova-Casadio), Archetype Publications, London, **2006**.
- [9] a) J. L. Mass, R. Oplia, B. Buckley, M. Cotte, J. Church, A. Mehta, *Appl. Phys. A: Mater. Sci. Process.* **2013**, *111*, 59-68; b) J. Mass, J. Sedlmair, C. S. Patterson, D. Carson, B. Buckley, C. Hirschmugl, *Analyst (Cambridge, U. K.)* **2013**, *138*, 6032-6043; c) E. Pouyet, M. Cotte, B. Fayard, M. Salomé, F. Meirer, A. Mehta, E. S. Uffelman, A. Hull, F. Vanmeert, J. Kieffer, M. Burghammer, K. Janssens, F. Sette, J. Mass, *Appl. Phys. A: Mater. Sci. Process.* **2015**, *121*, 967-980.
- [10] a) C. Miliani, A. Sgamellotti, K. Kahrin, B. G. Brunetti, A. Aldrovandi, M. R. van Bommel, K. J. van den Berg, H. Janssen, in *Preprints of the ICOM-CC 15th Triennial Meeting*, Vol. 2 (Ed. J. Bridgland), Allied Publishers Pvt Ltd, New Delhi/Mumbai/Kolkata, **2008**, pp. 244-251; b) A. Martins, C. Albertson, C. McGlinche, J. Dik, *Heritage Sci.* **2016**, *4*, 22.
- [11] a) J. K. Delaney, J. G. Zeibel, M. Thoury, R. Littleton, M. Palmer, K. M. Morales, E. René de la Rie, A. Hoenigswald, *Appl. Spectrosc.* **2010**, *64*, 584-594; b) K. Muir, A. Langley, A. Bezur, F. Casadio, J. Delaney, G. Gautier, *J. Am. Inst. Conserv.* **2013**, *52*, 156-172; c) P. A. Favero, J. Mass, J. K. Delaney, A. R. Woll, A. M. Hull, K. A. Dooley, A. C. Finnefrock, *Heritage Sci.* **2017**, *5*, 13.
- [12] a) F. Rosi, C. Grazia, R. Fontana, F. Gabrieli, L. Pensabene Buemi, E. Pampaloni, A. Romani, C. Stringari, C. Miliani, *Heritage Sci.* **2016**, *4*, 18; b) A. Martins, J. Coddington, G. Van der Snickt, B. van Driel, C. McGlinchey, D. Dahlberg, K. Janssens, J. Dik, *Heritage Sci.* **2016**, *4*, 33; c) Szafran, L. Rivers, A. Phenix, T. Learner, E. G. Landau, S. Martin, *Jackson Pollock's Mural: The Transitional Moment*, Getty Publications, Los Angeles, **2014**.
- [13] B. Leone, A. Burnstock, C. Jones, P. Hallebeek, J. Boon, K. Keune, *Preprints of the ICOM-CC 14th Triennial Meeting*, James & James, London, **2005**, pp. 803-813.
- [14] a) M. Lazzari, O. Chiantore, *Polym. Degrad. Stabil.* **1999**, *65*, 303-313; b) J. Mallégol, J. L. Gardette, J. Lemaire, *J. Am. Oil Chem. Soc.* **2000**, *77*, 257-263.
- [15] F. Rosi, L. Cartechini, L. Monico, F. Gabrieli, M. Vagnini, D. Buti, B. Doherty, C. Anselmi, B. G. Brunetti, C. Miliani, Tracking metal oxalates and carboxylates on painting surfaces by non-invasive reflection mid-FTIR spectroscopy, in: *Metal Soaps in Art - Conservation & Research* (Eds. F. Casadio, K. Keune, P. Noble, A. van Loon, E. Hendriks, S. Centeno, G. Osmond) Springer Nature book, **2018**, in press.
- [16] a) R. Mazzeo, S. Prati, M. Quaranta, E. Joseph, E. Kendix, M. Galeotti, *Anal. Bioanal. Chem.* **2008**, *392*, 65-76; b) J. Van der Weerd, A. van Loon, J. J. Boon, *Stud. Conserv.* **2005**, *50*, 3-22.
- [17] a) F. Gabrieli, F. Rosi, A. Vichi, L. Cartechini, L. Pensabene Buemi, S. G. Kazarian, C. Miliani, *Anal. Chem.* **2016**, *89*, 1283-1289, and references therein; b) J. J. Hermans, K. Keune, A. van Loon, P. D. Iedema, *J. Anal. At. Spectrom.* **2015**, *30*, 1600-1608.
- [18] a) S. Mauchauffee, E. Meux, M. Schneider, *Ind. Eng. Chem. Res.* **2008**, *47*, 7533-7537; b) M. S. Akanni, H. D. Burrows, H. A. Ellis, D. N. Asongwed, H. B. Babalola, P. O. Ojo, *J. Chem. Tech. Biotechnol.* **1984**, *34A*, 127-135.
- [19] B. Brunetti, C. Miliani, F. Rosi, B. Doherty, L. Monico, A. Romani, A. Sgamellotti, *Top. Curr. Chem.* **2016**, *374*, 10.
- [20] M. Fleet, *The Canadian Mineralogist* **2005**, *43*, 1811-1838.
- [21] M. A. Nasalevich, E. A. Kozlova, T. P. Lyubina, A. V. Vorontsov, *J. Catal.* **2012**, *287*, 138-148.
- [22] K. J. Green, R. Rudham, *J. Chem. Soc., Faraday Trans.* **1992**, *88*, 3599-3603.
- [23] J. J. Wang, Z. J. Li, X. B. Li, X. B. Fan, Q. Y. Meng, S. Yu, C. B. Li, J. X. Li, C. H. Tung, L. Z. Wu, *ChemSusChem* **2014**, *7*, 1468-1475.
- [24] H. Harada, T. Sakata, T. Ueda, *J. Phys. Chem.* **1989**, *93*, 1542-1548.
- [25] D. Meissner, R. Memming, B. Kastening, *J. Phys. Chem.* **1988**, *92*, 3476-3483.
- [26] A. E. Raevskaya, A. L. Stroyuk, S. Y. Kuchmii, *J. Nanopart. Res.* **2004**, *6*, 149-158.
- [27] J. Sabate, S. Cervera-March, R. Simarro, J. Giménez, *Chem. Eng. Sci.* **1990**, *45*, 3089-3096.
- [28] M. Gutierrez, A. Henglein, *Berichte der Bunsengesellschaft für physikalische Chemie* **1983**, *87*, 474-478.
- [29] H. Liu, H. Gao, M. Long, H. Fu, P. J. Alvarez, Q. Li, S. Zheng, X. Qu, D. Zhu *Environ. Sci. Technol.* **2017**, *51*, 6877-6886.
- [30] a) S. Chen, L. W. Wang, *Chem. Mater.* **2012**, *24*, 3659-3666; b) W. Anaf, O. Schalm, K. Janssens, K. De Wael, *Dyes Pigm.* **2015**, *113*, 409-415.
- [31] R. Wolbers, *Cleaning painted surfaces: aqueous methods*, Archetype Publications Ltd, London, **2000**.
- [32] A. J. Bard, M. S. Wrighton, *J. Electrochem. Soc.* **1977**, *124*, 1706-1710.
- [33] Y. A. Ilan, G. Czapski, D. Meisel *Biochim. Biophys. Acta, Bioenerg.* **1976**, *430*, 209-224.
- [34] W. Z. Tang, C. P. Huang, *War. Res.* **1995**, *29*, 745-756.
- [35] a) Z. J. Li, J. J. Wang, X. B. Li, X. B. Fan, Q. Y. Meng, K. Feng, B. Chen, C. H. Tung, L. Z. Wu *Adv. Mater.* **2013**, *25*, 6613-6618; b) T. Tachikawa, M. Fujitsuka, T. Majima, *J. Phys. Chem. C*, **2007**, *111*, 5259-5275; c) G. Liu, P. Niu, L. Yin, H. M. Cheng, *J. Am. Chem. Soc.* **2012**, *134*, 9070-9073.
- [36] A. P. Davis, Y. H. Hsieh, C. P. Huang *Chemosphere* **1995**, *31*, 3093-3104.
- [37] L. Maliy, G. Mokrousov, in *Solid State Phenomena*, Trans Tech Publications **2013**, pp. 175-178.
- [38] G. Liu, P. Niu, C. Sun, S. C. Smith, Z. Chen, G. Q. Lu, H. M. Cheng, *J. Am. Chem. Soc.* **2010**, *132*, 11642-11648.

- [39] a) J. C. Wu, J. Zheng, C. L. Zacherl, P. Wu, Z. K. Liu, R. Xu, *J. Phys. Chem. C* **2011**, *115*, 19741–19748; b) J. Lu, Y. Dai, M. Guo, W. Wei, Y. Ma, S. Han, B. Huang, *ChemPhysChem* **2012**, *13*, 147–154.
- [40] a) C. Xing, Y. Zhang, W. Yan, W., L. Guo, *Int. J. Hydrogen Energy* **2006**, *31*, 2018–2024; b) F. del Valle, A. Ishikawa, K. Domen, J. A. Villoria de la Mano, M. C. Sánchez-Sánchez, I. D. González, S. Herreras, N. Mota, M. E. Rivas, M. C. Álvarez Galván, J. L. G. Fierro, R. M. Navarro, *Catal. Today* **2009**, *143*, 51–56.
- [41] a) G. H. Völz, G. Kaempf, H. G. Fitzky, A. Klaeren, in *Photodegradation and Photostabilization of Coatings* (Eds: S. P. Pappas, F. H. Winslow), ACS symposium series, Vol. 151, American Chemical Society **1981**, pp. 163–182; b) P. A. Christensen, A. Dilks, T. A. Egerton, J. Temperley, *J. Mater. Sci.* **1999**, *34*, 5689–5700.
- [42] L. Monico, K. Janssens, M. Cotte, A. Romani, L. Sorace, C. Grazia, B. G. Brunetti, C. Miliani, *J. Anal. Atom. Spectrom.* **2015**, *30*, 1500–1510.
- [43] M. Cotte, E. Pouyet, M. Salome, C. Rivard, W. De Nolf, H. Castillo-Michel, T. Fabris, L. Monico, K. Janssens, T. Wang, P. Sciau, L. Verger, L. Cormier, O. Dargaud, E. Brun, D. Bugnazet, B. Fayard, B. Hesse, A. Pradas del Real, G. Veronesi, J. Langlois, N. Balcar, Y. Vandenberghe, V. A. Sole, J. Kieffer, R. Barrett, C. Cohen, C. Cornu, R. Baker, E. Gagliardini, E. Papillon, J. Susini, *J. Anal. Atom. Spectrom.* **2017**, *32*, 477–493.
- [44] C. G. Schroer, C. Baumbach, R. Dohrmann, S. Klare, R. Hoppe, M. Kahnt, J. Patommel, J. Reinhardt, S. Ritter, D. Samberg, M. Scholz, A. Schropp, F. Seiboth, M. Seyrich, F. Wittwer, G. Falkenberg, *AIP Conf. Proc.* **2016**, *1741*, 030007.

## Table of Contents

## FULL PAPER

**Why cadmium yellows ( $\text{CdS}/\text{Cd}_{1-x}\text{Zn}_x\text{S}$ ) are losing their color?** A combination of synchrotron radiation-based X-ray techniques, UV-visible and FTIR spectroscopies unveils the key-role played by moisture and light in the discoloration process of cadmium yellow oil paints. A mechanism for the photocorrosion of CdS-pigments and the photocatalytic oxidation process of the oil binder over CdS-particles upon variable moisture conditions is proposed (see Scheme).



Letizia Monico,\* Annalisa Chieli, Steven De Meyer, Marine Cotte, Wout de Nolf, Gerald Falkenberg, Koen Janssens, Aldo Romani, Costanza Miliani\*

Page No. – Page No.

**Role of relative humidity and Cd/Zn stoichiometry in the photo-oxidation process of cadmium yellows ( $\text{CdS}/\text{Cd}_{1-x}\text{Zn}_x\text{S}$ ) in oil paintings**